

Hg⁰ oxidative absorption by K₂S₂O₈ solution catalyzed by Ag⁺ and Cu²⁺

Xinhua Xu^{a,*}, Qunfeng Ye^{a,b}, Tingmei Tang^a, Dahui Wang^a

^a Department of Environmental Engineering, Zhejiang University, Hangzhou 310027, People's Republic of China

^b College of Chemistry & Life Science, Zhejiang Normal University, Jinhua 321004, People's Republic of China

Received 30 August 2007; received in revised form 25 January 2008; accepted 25 January 2008

Available online 8 February 2008

Abstract

The aqueous phase oxidation of gaseous elemental mercury (Hg⁰) by potassium persulfate (K₂S₂O₈, KPS) catalyzed by Ag⁺ and Cu²⁺ was investigated using a glass bubble column reactor. Concentrations of gaseous Hg⁰ and aqueous Hg²⁺ were measured by cold vapor generation atomic absorption spectrometry (CVAAS). The effects of several experimental parameters on the oxidation were studied; these include different types of catalysts, pHs and concentrations of potassium persulfate, temperatures, Hg⁰ inlet concentrations and tertiary butanol (TBA). The results showed that the removal efficiency of Hg⁰ increased with increasing concentration of potassium persulfate and catalysts Ag⁺, Cu²⁺ and Ag⁺ provided better catalytic effect than Cu²⁺. For example, in the presence of 5.0 mmol l⁻¹ KPS, the mercury removal efficiency could reach 75.4 and 97.0% for an Ag⁺ concentration of 0.1 and 0.3 mmol l⁻¹, respectively, and 69.8 and 81.9% for 0.1 and 0.3 mmol l⁻¹ Cu²⁺. On the other hand, high temperature and the introduction of TBA negatively affect the oxidation. Furthermore, the removal efficiency of Hg⁰ was much greater in neutral solution than in either acidic or alkaline solution. But the influence of pH was almost eliminated upon the addition of Ag⁺ and Cu²⁺, and high Hg⁰ inlet concentration also has positive impact on the removal efficiency of Hg⁰. The possible catalytic oxidation mechanism of gaseous mercury by KPS was also proposed.

© 2008 Elsevier B.V. All rights reserved.

Keywords: Potassium persulfate; Catalytic oxidation; Ag⁰; Absorption

1. Introduction

Mercury, a toxic agent present in trace amounts in coal and other potential fuels such as refuse-derived fuels and municipal solid wastes, will be released when these materials are burned. Lipfert et al. reported that methyl mercury level in edible fish doubled near a 1000 MW power plant [1]. On March 15, 2005, the US Environmental Protection Agency (EPA) issued the Clean Air Mercury Rule (CAMR) to permanently cap and reduce mercury emissions from coal-fired power plants because of its volatility, persistence and bioaccumulation as methyl mercury in the environment and its neurological health impacts. Coal-fired utility boilers are now identified as the largest source of mercury in the United States [2,3], releasing approximately 50 tons of mercury annually or about one-third of the total anthropogenic emission. The concentration of mercury from coal-fired flue gases was at the level of several tens of microgrammes per cubic meter.

In China, coal now accounts for about 67% of the primary energy consumption and will continue to play an important role in energy uses for a long time to come. The total amount of coal consumption is about 2.3 billion tons in 2006. Although there is no direct evidence of health problems caused by Hg released from Chinese coals, a high Hg concentration in the atmosphere from coal combustion has been reported [4].

Hg⁰ is practically water insoluble and hence difficult to capture, however, Hg²⁺ is water-soluble and can be efficiently removed in wet scrubbers, which exhibit up to 90% removal of Hg²⁺. So, it is necessary to use oxidizers to remove gaseous Hg⁰ by transforming it into Hg²⁺. The standard potential of the redox-pair Hg⁰/Hg²⁺ is 0.85 V. To achieve complete reaction, the over-potential should be 0.3–0.4 V. Therefore, the standard oxidizing potential of the oxidizers applied should at least be 1.2 V [5]. Some oxidizers meeting the above requirement include: KMnO₄, K₂S₂O₈, K₂CrO₇, H₂O₂, NaClO₄, NaClO₃ or Cl₂ [5–11]. The standard oxidizing potential of potassium persulfate (KPS) is 2.01 V, which is higher than that of potassium permanganate (1.7 V). The general catalysts found in the literature include copper and silver ions [11], manganese [11–13], cerium [11,14] and cobalt [12]. Liang et al. studied persulfate

* Corresponding author. Tel.: +86 571 87951239; fax: +86 571 87952771.
E-mail address: xuxinhua@zju.edu.cn (X. Xu).

oxidation in situ remediation of trichloroethylene (TCE) catalyzed by ferrous ion [15,16].

Currently, there is limited information on the possible mechanism of the reaction between Hg^0 and potassium persulfate in the literature. In this study, the feasibility of Hg^0 absorption in potassium persulfate catalyzed by Ag^+ and Cu^{2+} was evaluated in a bubble column reactor. This study was aimed at determining the removal efficiency of Hg^0 in solution under different conditions. Towards the end, the mechanism of the reaction between Hg^0 and potassium persulfate in the process was also hypothesized. Recently, efforts are being taken to investigate the reaction mechanism for homogeneous Hg^0 oxidation through a sequence of fundamental reactions, such as the method of mercury removal from coal combustion by Fenton reactions developed at the CANMET Energy Technology Centre for Hg removal from coal combustion, and so far, both bench- and pilot-scale tests have been carried out to evaluate its effectiveness. So, this technique also can be applied to oxidize Hg^0 to Hg^{2+} from the coal or waste incineration flue gas in practice.

2. Experiments and methods

2.1. Chemicals

Mercury permeation tube (USA VICI Metronics), potassium persulfate (>99.5%, AR), hydroxylamine hydrochloride (>98.5%, AR), nitric acid (GR), hydrochloric acid (GR), sulfuric acid (GR), sodium hydroxide (>98.0%, GR), stannous chloride (>98.0%, CP), stannum (>99.9%, AR), potassium permanganate (>99.5%, GR), potassium dichromate (>99.8%, GR), mercury chloride (>99.0%, AR), silver nitrate (>99.8%, AR), anhydrous sodium carbonate (>99.8%, AR), sodium bicarbonate (>99.5%, AR), acetone (>99.5%, AR) and tertiary butanol (CP) were all purchased from Shanghai Chemical Reagents Co., and used without further purification.

2.2. Batch experiment procedures

All batch experiments were performed in a 500 ml bubble column reactor equipped with a glass gas frit at the bottom (shown in Fig. 1) with an available volume of 300 ml solution in a water bath, which can change the reaction temperature. The top of the reactor had two openings providing connections to a pipette for

feeding or sampling and for venting the gas. All connections including tubing and valves were composed of either Teflon or glass without metals. The pipes between U-tube and reactor were packed with resistance coils to provide proper insulation for temperature control.

The Hg generator was heated (both elemental and oxidized Hg permeation tubes). The Hg generator was supplied from a permeation tube inside a glass U-tube, immersed in one water bath (T_1) at a pure nitrogen flow of 120 ml min^{-1} . The total flow (G) was 11 min^{-1} diluted by nitrogen, the inlet concentration of Hg^0 is $50\text{--}60 \mu\text{g m}^{-3}$. In each typical experiment, the temperature of water baths was adjusted to the constant values, and then 250 ml water or other background solution was put into the reactor being immersed in the other water bath (T_2). Finally, a Hg^0/N_2 gas mixture was passed over the solution in the reactor and the vent gas was scrubbed by acidic KMnO_4 . After about 2 h, the mixed gas was passed over 10% (v/v) H_2SO_4 –4% (w/w) KMnO_4 solution adopted by Environmental Protection Agency (EPA), 10 ml each, inside two impingers in series for 1 min. Then the vent gas was switched to waste gas scrubber again. The process was repeated three times at 10 min intervals. The average value was then recorded as the initial Hg^0 concentration in the inlet.

If these three values gave stable readings, the Hg^0 oxidative absorption experiments by $\text{K}_2\text{S}_2\text{O}_8$ solution began. The $\text{K}_2\text{S}_2\text{O}_8$ solution was sequentially injected into the reactor using a syringe with a slim Teflon tube. The outlet mercury was also extracted using the prepared KMnO_4 – H_2SO_4 solutions and the outlet Hg concentration was analyzed by QM201B mercury analyzer.

The percent of Hg^0 removal efficiency was determined by the following equation:

$$\% \text{removal} = 100 \times \frac{\text{Hg}_{(\text{inlet})}^0 - \text{Hg}_{(\text{outlet})}^0}{\text{Hg}_{(\text{inlet})}^0} \quad (1)$$

2.3. Analytical methods

Liquid samples (after extracted from the prepared KMnO_4 – H_2SO_4 solutions) in two impingers were put into the test tubes. Before analysis, several drops of hydroxylamine hydrochloride were added into the test tubes until the solution color turned clear to reduce the extra KMnO_4 , and fix the value, after holding still for 10 min, 5 ml sample was then transferred into a mercury detecting bottle, an accessory of QM201B mercury analyzer (Qingan Instrument Co., Suzhou, China), and 1 ml 10% (w/w) SnCl_2 solution was added in order to reduce Hg^{2+} to Hg^0 , mercury vapor produced was supplied with a N_2 carrier gas and flushed into atomic absorption spectrometry.

The samples were periodically collected by glass syringes at selected time intervals, filtered twice through $0.22 \mu\text{m}$ membrane filters and then analyzed for sulfate using a Metrohm 792 Basic Ion Chromatograph (IC) equipped with a Metrosep A Supp 4 column ($250 \text{ mm} \times 4.0 \text{ mm}$), a Metrosep A Supp 4/5 guard column, and a conductivity detector. Sodium carbonate (2.0 mM) and sodium bicarbonate (1.0 mM) served as eluents.

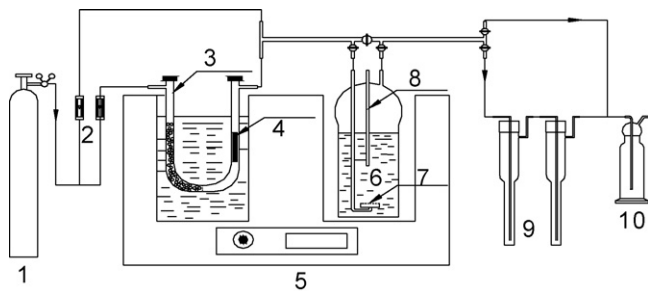


Fig. 1. Schematic diagram of the experimental apparatus. (1) N_2 , (2) rotameter, (3) U-tube, (4) mercury permeation tube, (5) water bath, (6) reactor, (7) gas diffuser, (8) sample out, (9) impinger and (10) waste gas scrubber.

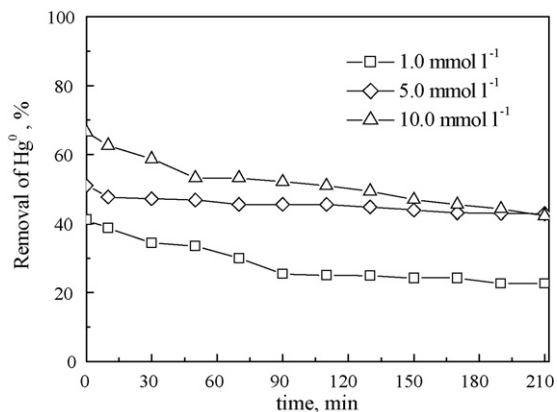


Fig. 2. Effect of KPS addition on the Hg⁰ removal efficiency. pH 7, $T_1 = 50^\circ\text{C}$, $T_2 = 55^\circ\text{C}$, $G = 1.01\text{ min}^{-1}$.

And pH value was measured with a digital pH meter (JENCO, Shanghai, China).

3. Results and discussion

3.1. Effect of $\text{K}_2\text{S}_2\text{O}_8$ concentration

The mercury removal profiles with different initial potassium persulfate concentration in the absence of any catalysts are shown in Fig. 2. Evidently, Hg⁰ concentration at the reactor outlet decreases sharply at the beginning, and then reaches a plateau nearly as the reaction continues, probably due to the presence of excess KPS. The highest reaction rate was found to correlate with the highest initial concentration of KPS. For instance, at the beginning the removal efficiency of mercury reached 41.1 and 66.5% when the potassium persulfate concentrations were 1.0 and 5.0 mmol l⁻¹, after a reaction time of 210 min, the removal rate of mercury reached 22.6 and 42.1%, respectively.

3.2. Effect of Ag^+ and Cu^{2+} concentration

As shown in Figs. 3 and 4, the addition of Cu^{2+} and Ag^+ accelerates dramatically the reaction rate and increases the mercury removal efficiency due to the production of high

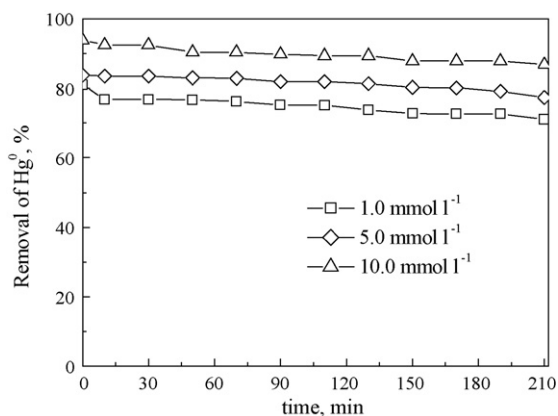


Fig. 3. Effect of KPS concentrations on the Hg⁰ catalytic removal efficiency. pH 7, $T_1 = 50^\circ\text{C}$, $T_2 = 55^\circ\text{C}$, $G = 1.01\text{ min}^{-1}$ and $\text{Cu}^{2+} = 0.5\text{ mmol l}^{-1}$.

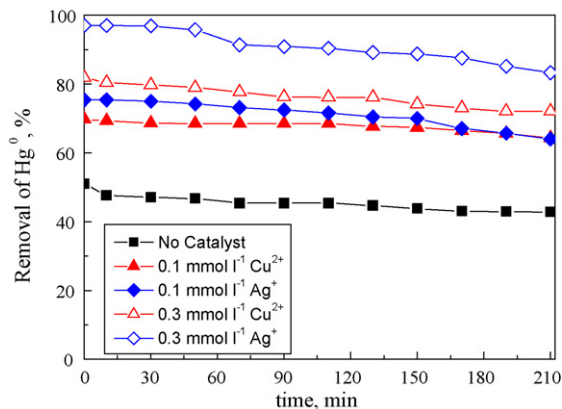


Fig. 4. Effect of catalysts concentration on the Hg⁰ removal efficiency. pH 7, $T_1 = 50^\circ\text{C}$, $T_2 = 55^\circ\text{C}$, $G = 1.01\text{ min}^{-1}$ and $C_{\text{KPS}} = 5.0\text{ mmol l}^{-1}$.

reactive transition ions. When the Cu^{2+} concentration was 0.5 mmol l⁻¹, the removal efficiency of mercury reached 81.1, 83.8 and 93.9% with an initial KPS concentration of 1.0, 5.0 and 10.0 mmol l⁻¹, respectively. In contrary, the mercury removal efficiency reached only 41.1, 51.0 and 66.5% in the absence of catalysts, respectively. Furthermore, Ag^+ provided better catalytic effect than Cu^{2+} , the mercury removal efficiency could reach 75.4 and 97.0% corresponding to 0.1 and 0.3 mmol l⁻¹ Ag^+ for 5.0 mmol l⁻¹ KPS, respectively, and just 69.8 and 81.9% corresponding to 0.1 and 0.3 mmol l⁻¹ Cu^{2+} at the beginning. The results also show that 0.1 mmol l⁻¹ AgNO_3 is not enough to remove mercury completely for 5.0 mmol l⁻¹ KPS. The greater the silver nitrate concentration is, the higher the mercury removal rate was found in our study. This observation agrees very well with a report previously published by others, in which the reaction rate was found to be proportional to the KPS concentration and to the AgNO_3 concentration [11].

3.3. Effect of initial pH value

Fig. 5 shows the influence of initial pH value on the Hg⁰ removal. While initial pH was 7.0, the removal efficiency of Hg⁰ reached nearly 60.4% at the beginning, followed by 37.2% for 1 mol l⁻¹ HNO_3 solution (pH is about 0.1). While NaOH concentration was 0.1 mol l⁻¹ (pH is about 13), Hg⁰ removal efficiency was extremely low, and reached no more than 12.9%. After 40 min, the removal efficiency of Hg⁰ descended to 54.4, 30.8 and 5.5%, respectively. It was obvious that the presence of both H^+ and OH^- , especially OH^- , greatly weakened the Hg⁰ oxidation when silver nitrite was absent.

The decomposition of $\text{S}_2\text{O}_8^{2-}$ could be catalyzed by acid. The reaction mechanism could be explained by the following reactions [11]:



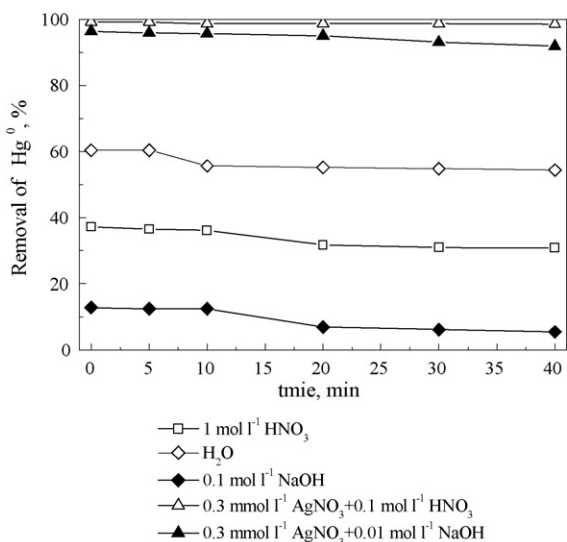
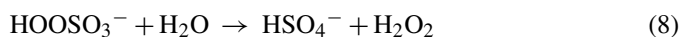
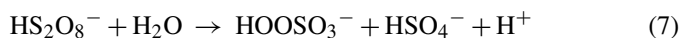
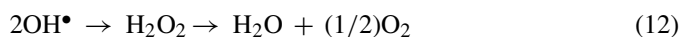
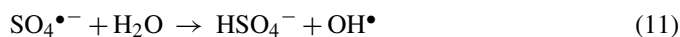
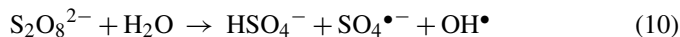


Fig. 5. Effect of pH on the Hg⁰ removal efficiency. $T_1 = 50^\circ\text{C}$, $C_{\text{KPS}} = 10.0 \text{ mmol l}^{-1}$, $T_2 = 25^\circ\text{C}$ and $G = 1.01 \text{ min}^{-1}$.

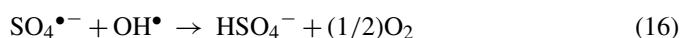
$\text{S}_2\text{O}_8^{2-}$ also could be hydrolyzed and form H_2O_2 as following reactions:



First of all, $\text{S}_2\text{O}_8^{2-}$ may be decomposed unsymmetrically by its reaction with acidic H_2O because of the influence of H^+ , which leads to the breaking of the O–S bond. On the other hand, $\text{S}_2\text{O}_8^{2-}$ can also react with H_2O in neutral solutions to produce $\text{SO}_4^{\bullet-}$ (Eq. (9)), a reaction which was considered the rate-limiting step [11]. In this step, $\text{S}_2\text{O}_8^{2-}$ was decomposed to form $\text{SO}_4^{\bullet-}$ by breaking of the O–O bond.



$\text{S}_2\text{O}_8^{2-}$ also can be decomposed as following:



So free radicals can produce in neutral solutions. On the contrary, no or little available species are produced in acidic aqueous solutions. Dogliotti and Hayon reported that sulfate radicals dominated in the photolysis of persulfate ions in neutral and acidic aqueous solutions [17]. However, in alkaline solutions, sulfate radicals are converted into hydroxyl radicals (OH^\bullet). It

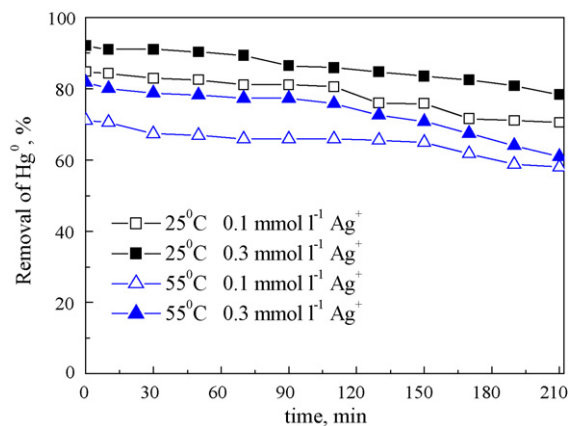


Fig. 6. Effect of reaction temperature on the Hg⁰ removal efficiency. pH 7, $T_1 = 50^\circ\text{C}$, $C_{\text{KPS}} = 1.0 \text{ mmol l}^{-1}$ and $G = 1.01 \text{ min}^{-1}$.

was shown that sulfate radicals (2.5–3.1 V) are stronger oxidants than hydroxyl radicals (1.985, 2.38 or 2.72 V in acidic solution), especially at elevated pH [18,19]. But the results in alkaline solutions, under which KPS would not decompose easily due to the lack of available H_2O or H^+ , indicated that no free radicals were produced without light. But the difference was largely eliminated by the addition of Ag^+ , regardless of acid or alkaline solutions.

3.4. Effect of reaction temperature

Fig. 6 demonstrates the effect of reaction temperature T_2 on Hg⁰ removal, our results suggest that the Hg⁰ removal efficiency decreases with increasing reaction temperature, while lower temperature enhances the mercury removal. At the beginning, the removal efficiency was reduced from 84.8, 92.0% at 25°C to 71.1, 81.7% at 55°C for 0.1 mmol l^{-1} and 0.3 mmol l^{-1} AgNO_3 with 1.0 mmol l^{-1} KPS, respectively. The energy of O–O bond is 33.5 kJ mol^{-1} and the activation energy is $(121 \pm 12) \text{ kJ mol}^{-1}$ for the decomposition of KPS [20], which is in reasonable agreement with 130 kJ mol^{-1} as reported in a previous work when potassium persulfate decomposed to radical $\text{SO}_4^{\bullet-}$ whose potential was as high as 2.6 V [21]. Due to the high activation energy, the reaction rate is quite slow at room temperature and acceptable rate can only be achieved over 50°C . But the rate constant of $\text{SO}_4^{\bullet-}$ recombination is $(2.7 \pm 0.2) \times 10^9 \text{ l mol}^{-1} \text{ s}^{-1}$ [22], which is the same order as compared to OH^\bullet recombination ($5.5 \times 10^9 \text{ l mol}^{-1} \text{ s}^{-1}$), which is also affected by the reaction temperature. But the efficiency of KPS/ AgNO_3 is comparable with that of $\text{KMnO}_4/\text{H}_2\text{SO}_4$ as oxidants for Hg⁰ removal. The latter reaction rate is in the range of $10^7 \text{ l mol}^{-1} \text{ s}^{-1}$ [8]. As a result, the effect of reaction temperature was investigated from two inverse aspects. One is that high temperature can elevate the reaction rate, but also restrain the reaction because of free radical recombination as a result of the temperature raise. Furthermore, the net effect is governed by the latter according to our experiment results, so the optimal temperature should be lower than 50°C in the actual absorption reactions.

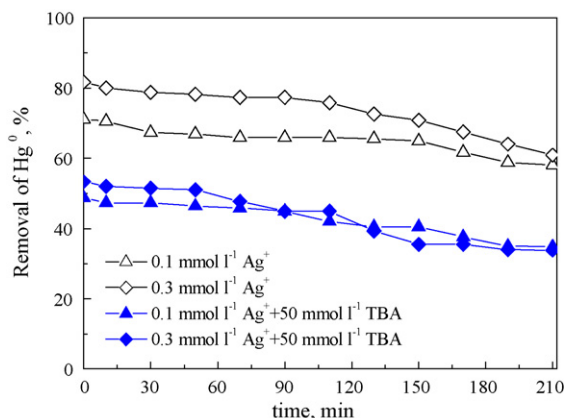


Fig. 7. Effect of TBA on the Hg⁰ removal efficiency. pH 7, $T_1 = 50^\circ\text{C}$, $C_{\text{KPS}} = 1.0 \text{ mmol l}^{-1}$, $T_2 = 55^\circ\text{C}$ and $G = 1.01 \text{ min}^{-1}$.

3.5. Effect of TBA

Fig. 7 gives the results about the effect of TBA on mercury removal. Generally speaking, radical scavengers include mainly CO_3^{2-} and HCO_3^{2-} and TBA, which react with $\text{OH}\cdot$ at rates of 4.2×10^8 , 1.5×10^7 and $5.0 \times 10^8 \text{ l mol}^{-1} \text{ s}^{-1}$ respectively [23]. Among them, TBA is the most active one. To ascertain whether $\text{OH}\cdot$ and $\text{SO}_4^{\bullet-}$ were involved in the reaction between Hg⁰ and potassium persulfate, 50 mmol l⁻¹ TBA was put into the solution. According to Fig. 7, at the beginning, the removal efficiency of mercury descend to 48.8 and 53.3% for 0.1 and 0.3 mmol l⁻¹ AgNO₃ with the addition of 50 mmol l⁻¹ TBA from 71.1 and 81.7% without the TBA addition. The removal efficiency of mercury reached 33.8 and 34.8%, after 210 min reaction, also was lower about 15–20% than the removal efficiency without TBA addition, which was attributed to the influence of TBA. So it can be concluded that the role of free radicals could be significant in the reaction.

3.6. Reaction mechanism

It was postulated that persulfate anion ($\text{S}_2\text{O}_8^{2-}$) can be thermally or chemically catalyzed by transition metal ions to produce a powerful oxidant known as the sulfate free radical ($\text{SO}_4^{\bullet-}$) [11], which can extract hydrogen from water to give hydroxyl radicals ($\text{OH}\cdot$) and potentially destroy organic contaminants within the soil mass by in situ chemical oxidation.

The roles of free radicals and transition metal ions in the reaction were investigated by adding 50 mmol l⁻¹ TBA as discussed above, which proved the postulation. Fig. 8 indicates that the production of SO_4^{2-} almost linearly increases, while pH decreases with time.

The reactions of persulfate ions with various organic and inorganic compounds have been extensively studied [11,21,24]. Persulfate oxidation is generally conducted under heat-, photo- or metal-catalyzed conditions because the oxidation rates can be greatly accelerated. Highly reactive species such as sulfate radicals ($\text{SO}_4^{\bullet-}$) and hydroxyl radicals ($\text{OH}\cdot$) are generated as a result of photolysis or heat decomposition of persulfate ions in aqueous phases [17,24–27]. And sulfate radicals are

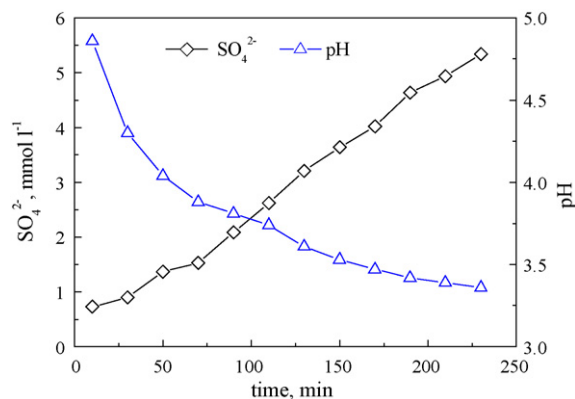
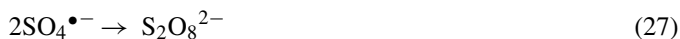
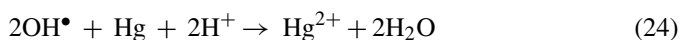
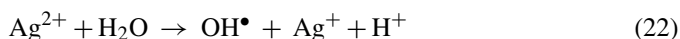
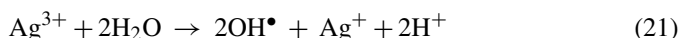


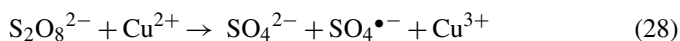
Fig. 8. Transformation plot of sulfate anion and pH as a function of time. pH 7, $T_1 = 50^\circ\text{C}$, $T_2 = 55^\circ\text{C}$, $C_{\text{KPS}} = 5.0 \text{ mmol l}^{-1}$, $C_{\text{CN}} = 0.3 \text{ mmol l}^{-1}$ and $G = 1.01 \text{ min}^{-1}$.

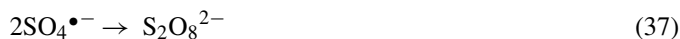
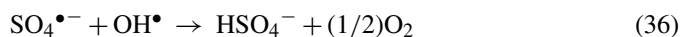
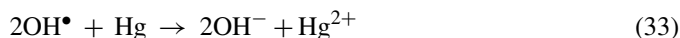
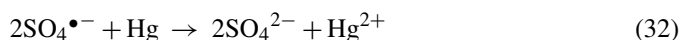
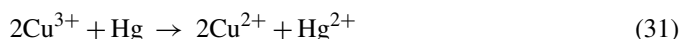
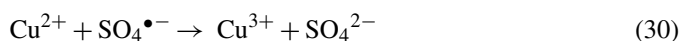
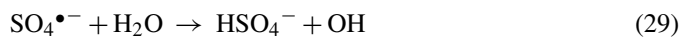
stronger oxidants than hydroxyl and the thermodynamics of the transition-metal-oxidant coupling [18,19], since they are more selective for oxidation (electron transfer). Hydroxyl radicals may react rapidly also by the removal and addition of hydrogen, which was also evidenced from our observation.

However, persulfate oxidation at atmospheric temperature is usually not effective. Persulfate is commonly used with UV light, catalyzed by transition metals or under high temperature in order to initiate or enhance its radical oxidation mechanisms (as Eqs. (17)–(27) show). Sulfate radicals, formed from heat or chemically catalyzed by silver ion decomposition of persulfate (Eq. (17)), may initiate a series of radical-transfer chain reactions (Eqs. (18)–(22)) [24] where elemental mercury (Eqs. (23) and (24)) is mainly removed. At the same time, instable transition species (Ag^{3+} and Ag^{2+}) probably also contribute to mercury removal via $\text{OH}\cdot$ formation. Chain termination occurs in some situations to result in radical recombination (Eqs. (25) and (27)).



Sulfate radicals, formed from heat or chemically catalyzed by Cu^{2+} decomposition of persulfate, may initiate a series of radical-transfer chain reactions (Eqs. (28)–(37)).





The most probable reaction stoichiometry between Hg^0 and KPS is 1:1, as shown below:



After 210 min, the reaction was fully complete, it was only $1.75 \times 10^{-4} \text{ mmol l}^{-1}$ KPS concentration that could reach the theoretical value. Obviously, 5.0 mmol l^{-1} KPS was excess. Fig. 7 shows that 2.67 mmol l^{-1} KPS was consumed, which accounted for 53.4%. These results may be explained by the facts that free radicals would recombine or react with other reagents instead of Hg^0 , and that, as a result, chain reaction ceased. The other reason may be that the decomposition of KPS (being catalyzed by Ag^+) continued to proceed without any pretreatment before IC analysis.

4. Conclusions

Research has been conducted to characterize and modify Hg species (through conversion of Hg^0 to Hg^{2+}) in gases so that a Hg^0 control strategy can be implemented in a wet scrubber. Hg^0 removal efficiency increases with the increasing concentration of potassium persulfate and catalysts, and decreases with the addition of TBA. Ag^+ provided better catalytic effect than Cu^{2+} , the mercury removal efficiency could reach 75.4 and 97.0% corresponding to 0.1 and 0.3 mmol l^{-1} Ag^+ for 5.0 mmol l^{-1} KPS, respectively, and just 69.8 and 81.9% corresponding to 0.1 and 0.3 mmol l^{-1} Cu^{2+} . Hg^0 oxidation by $\text{K}_2\text{S}_2\text{O}_8$ may be achieved simultaneously via two different processes, namely, direct oxidation by $\text{K}_2\text{S}_2\text{O}_8$ and indirect reaction by free radicals. $\text{K}_2\text{S}_2\text{O}_8$ is decomposed into $\text{SO}_4^{\bullet-}$, which oxidize metal ions to highly reactive valent species and H_2O to OH^{\bullet} . Both of them oxidize Hg^0 quickly to Hg_2^{2-} , which can be oxidized to the final product, Hg^{2+} , in solutions.

Acknowledgements

This research was supported by the National High Technology Research and Development Program of China (No. 2007AA06Z340) and the Program for New Century Excellent Talents in University (No. NCET-06-0525).

References

- [1] F.W. Lipfert, P.D. Moskowitz, V. Fterakis, M. Dephillips, J. Viren, L. Saroff, Assessment of adult risks of paresthesia due to mercury from coal combustion, *Water Air Soil Poll.* 80 (1995) 1139–1148.
- [2] US EPA, Mercury Study Report to Congress EPA-452/R-97-003, US EPA Office of Air Quality Planning and Standards, US Government Printing Office, Washington, DC, 1997.
- [3] US EPA, A Study of Hazardous Air Pollutant Emissions from Electric Utility Steam Generating Units: Final Report to Congress, EPA-453/R-98-004a, US EPA Office of Air Quality Planning and Standards, US Government Printing Office, Washington, DC, 1998.
- [4] L.G. Zheng, G.J. Liu, C.L. Chou, The distribution, occurrence and environmental effect of mercury in Chinese coals, *Sci. Total Environ.* 384 (2007) 374–383.
- [5] R. van der Vaart, J. Akkerhuis, P. Feron, B. Jansen, Removal of mercury from gas streams by oxidative membrane gas absorption, *J. Membr. Sci.* 187 (2001) 151–157.
- [6] A.I. Martinez, B.K. Deshpande, Kinetic modeling of H_2O_2 -enhanced oxidation of flue gas elemental mercury, *Fuel Process. Technol.* 88 (2007) 982–987.
- [7] H. Morita, T. Mitsuhashi, H. Sakurai, S. Shimomura, Absorption of mercury by solutions containing oxidants, *Anal. Chim. Acta* 153 (1983) 351–355.
- [8] L.L. Zhao, G.T. Rochelle, Hg absorption in aqueous permanganate, *AIChE J.* 42 (1996) 3559–3562.
- [9] L.L. Zhao, G.T. Rochelle, Mercury absorption in aqueous oxidants catalyzed by mercury(II), *Ind. Eng. Chem. Res.* 37 (1998) 380–387.
- [10] L.L. Zhao, G.T. Rochelle, Mercury absorption in aqueous hypochlorite, *Chem. Eng. Sci.* 54 (1999) 655–662.
- [11] D.A. House, Kinetics and mechanism of oxidations by peroxydisulfate, *Chem. Rev.* 62 (1962) 185–203.
- [12] S. Lenka, S.B. Dash, Polymerization of acrylonitrile initiated by potassium persulfate-cobalt(II) and potassium persulfate-manganese(II) redox system, *J. Macromol. Sci. Chem. A* 20 (1983) 397–407.
- [13] V.N. Kislenco, A.A. Berlin, N.V. Litovchenko, Kinetics of oxidation of glucose by persulfate ions in the presence of Mn(II) ions, *Kinet. Catal.* 38 (1997) 391–396.
- [14] J. Skarzewski, Cerium catalyzed persulfate oxidation of polycyclic aromatic hydrocarbons to quinines, *Tetrahedron* 40 (1984) 4997–5000.
- [15] C.J. Liang, C.J. Bruell, M.C. Marley, K.L. Sperry, Persulfate oxidation for in situ remediation of TCE. I. Catalyzed by ferrous ion with and without a persulfate-thiosulfate redox couple, *Chemosphere* 55 (2004) 1213–1223.
- [16] C.J. Liang, C.J. Bruell, M.C. Marley, K.L. Sperry, Persulfate oxidation for in situ remediation of TCE. II. Catalyzed by chelated ferrous ion, *Chemosphere* 55 (2004) 1225–1233.
- [17] L. Dogliotti, E. Hayon, Flash photolysis of persulfate ions in aqueous solutions. Study of the sulfate and ozonide radical anions, *J. Phys. Chem.* 71 (1967) 2511–2516.
- [18] G.P. Anipistakis, D.D. Dionysiou, Transition metal/UV-based advanced oxidation technologies for water decontamination, *Appl. Catal. B: Environ.* 54 (2004) 155–163.
- [19] G.P. Anipistakis, D.D. Dionysiou, Degradation of organic contaminants in water with sulfate radicals generated by the conjunction of peroxymonosulfate with cobalt, *Environ. Sci. Technol.* 37 (2003) 4790–4797.
- [20] G.J. Price, A.A. Clifton, Sonochemical acceleration of persulfate decomposition, *Polymer* 37 (1996) 3971–3973.
- [21] I.M. Kolthoff, I.K. Miller, The chemistry of persulfate. I. The kinetics and mechanism of the decomposition of the persulfate ion in aqueous medium, *J. Am. Chem. Soc.* 73 (1951) 3055–3059.
- [22] K.L. Ivanov, E.M. Glebov, V.F. Plyusnin, Y.V. Ivanov, V.P. Grivin, N.M. Bazhin, Laser flash photolysis of sodium persulfate in aqueous solution with additions of dimethylformamide, *J. Photochem. Photobiol. A* 133 (2000) 99–104.
- [23] B. Langlais, D.A. Reckhow, D.R. Brink, *Ozone in Water Treatment – Applications and Engineering*, Lewis Publishers, Chelsea, 1991.

- [24] A.A. Berlin, Kinetics of radical-chain decomposition of persulfate in aqueous solutions of organic compounds, *Kinet. Catal.* 27 (1986) 34–39.
- [25] E.F. Nosov, Rate constant determination in the decomposition of potassium and ammonium peroxydisulfate in aqueous solution, *Russ. J. Phys. Chem.* 40 (1966) 1571–1572.
- [26] E. Hayon, J.J. McGarvey, Flash photolysis in the vacuum ultraviolet region of OH^- ions in aqueous solutions, *J. Phys. Chem.* 71 (1967) 1472–1477.
- [27] D.D. Tanner, S.A.A. Osman, Oxidative decarbonation on the mechanism of potassium persulfate promoted decarbonation reaction, *J. Org. Chem.* 52 (1987) 4689–4693.